

RETHINKING THE POWER OF GRAPH CANONIZATION IN GRAPH REPRESENTATION LEARNING WITH STABILITY

Zehao Dong¹ Muhan Zhang² Philip R.O. Payne¹ Michael A Province¹

Carlos Cruchaga¹ Tianyu Zhao¹ Fuhai Li¹ Yixin Chen¹

¹ Washington University in St. Louis

² Institute for Artificial Intelligence, Peking University

{zehao.dong, prpayne, mprovince, cruchagac, tzhao, fuhai.li}@wustl.edu
chen@cse.wustl.edu & muhan@pku.edu.cn

ABSTRACT

The expressivity of Graph Neural Networks (GNNs) has been studied broadly in recent years to reveal the design principles for more powerful GNNs. Graph canonization is known as a typical approach to distinguish non-isomorphic graphs, yet rarely adopted when developing expressive GNNs. This paper proposes to maximize the expressivity of GNNs by graph canonization, then the power of such GNNs is studied from the perspective of model stability. A stable GNN will map similar graphs to close graph representations in the vectorial space, and the stability of GNNs is critical to generalize their performance to unseen graphs. We theoretically reveal the trade-off of expressivity and stability in graph-canonization-enhanced GNNs. Then we introduce a notion of universal graph canonization as the general solution to address the trade-off and characterize a widely applicable sufficient condition to solve the universal graph canonization. A comprehensive set of experiments demonstrates the effectiveness of the proposed method. In many popular graph benchmark datasets, graph canonization successfully enhances GNNs and provides highly competitive performance, indicating the capability and great potential of proposed method in general graph representation learning. In graph datasets where the sufficient condition holds, GNNs enhanced by universal graph canonization consistently outperform GNN baselines and successfully improve the SOTA performance up to 31%, providing the optimal solution to numerous challenging real-world graph analytical tasks like gene network representation learning in bioinformatics.

1 INTRODUCTION

Graph Neural Networks (GNNs) (Kipf & Welling, 2016; Hamilton et al., 2017; Xu et al., 2019; Velickovic et al., 2018; You et al., 2018; Scarselli et al., 2008; Duvenaud et al., 2015; Gilmer et al., 2017; Zhang et al., 2018) are dominant architectures for modeling the relational structured data. GNNs implicitly leverage the inductive bias in the graph topology by iteratively passing messages between nodes to extract a node embedding that encodes the local substructure, showing great expressivity and scalability to extract representative features for graph learning problems. Due to the superior representation ability and scalability, GNNs have achieved impressive results on various graph-structured data, such as social networks (Monti et al., 2017; Ying et al., 2018), protein networks (Fout, 2017; Zitnik et al., 2018) and circuit networks (Dong et al., 2022a).

Numerous efforts (Xu et al., 2019; Morris et al., 2019) have been put in analyzing the effectiveness of GNNs and indicate that popular GNNs, which mimic the 1-dimensional Weisfeiler-Lehman (1-WL) algorithm/color refinement algorithm (Leman & Weisfeiler, 1968), suffer from the limitations of 1-WL in the expressive power. Hence, the dominant approach to enhance the performance of GNNs is to improve their expressivity. Informally, recent powerful GNNs achieve this purpose from four perspective. (1) High-order GNNs (Morris et al., 2019; Maron et al., 2019) mimic the higher-order WL tests to improve the expressivity beyond 1-WL; (2) Subgraph-based GNNs (Zhang & Li, 2021; You et al., 2021; Bevilacqua et al., 2021) encode (learnable) local structures (i.e. induced

k-hop neighborhoods) of nodes, thus formulating hierarchies of local isomorphism on neighborhood subgraphs to beat 1-WL. (3) GNNs with markings (Papp et al., 2021) slightly perturb the input graphs for multiple times to execute GNNs and then aggregates the final embeddings of these perturbed graphs in each run. (4) Feature augmentation GNNs (Abboud et al., 2020; Lim et al., 2022) add pre-computed/learned node features to improve the expressivity. Overall, these expressive GNNs are powerful, yet still far from efficiently distinguishing any pair of nonisomorphic graphs. For instance, high-order GNNs and GNNs with markings are not scalable to large-scale graphs due to the space and time complexity, while subgraph-based GNNs have an upper bounded expressivity as there always exists graphs (Papp & Wattenhofer, 2022) distinguishable by 2-WL (3-WL) yet not distinguishable by subgraph-based GNNs.

Graph canonization generates the canonical form of a graph G that is isomorphic to any graph in its isomorphic group $ISO(G)$, then any two graphs are distinguishable by checking whether their canonical forms are identical. Thus, graph canonization maximizes the discriminating ability of non-isomorphic graphs. As for the concern of the complexity, though the determination of the canonical form of a graph is shown to be NP-hard Babai & Luks (1983), canonization tools such as Nauty (McKay & Piperno, 2014) can effectively find the canonical form of a reasonable-sized graph. For instance, Nauty has an average time complexity of $O(n)$, and polynomial-time graph canonization algorithms also exist for graphs of bounded degrees. Hence, we propose to enhance GNNs with graph canonization.

The positional encoding scheme (Vaswani et al., 2017) is introduced in the sequence encoding problem to describe the position of an entity in a sequence so that each position is associated with a unique representation. In recent years, it is widely adopted in graph Transformers (Yan et al., 2020; Dong et al., 2022b), and we resort to this scheme when applying graph canonization in GNNs. For a graph G with node set $V = \{v_1, v_2, \dots, v_n\}$, the graph canonization finds a bijective function $\rho(v|G)$ from V onto $\{1, 2, \dots, n\}$ such that the canonical form of G can be obtained by reordering nodes according to the generated discrete colouring $\{\rho(v_1|G), \rho(v_2|G), \dots, \rho(v_n|G)\}$. Since isomorphic graphs have the same canonical form, function $\rho(v|G)$ provides a unique way to label nodes in graphs from the same isomorphic group $ISO(G)$. Thus, our proposed graph-canonization-enhanced GNNs take one-hot encodings of $\{\rho(v_1|G), \rho(v_2|G), \dots, \rho(v_n|G)\}$ as nodes' positional encodings, which help to maximize the expressive power in graph classification.

In the design of deep learning models, the generalization behavior (Hardt et al., 2016; Bartlett et al., 2017) also plays a critical role for competitive performance. Inspired by Wang et al. (2022), we study how well GNNs are generalized to unseen graphs with the model stability. Informally, a stable GNN can map similar graphs to close graph representations in the vectorial space. In the graph canonization problem, similar graphs may have complete different discrete colourings $\{\rho(v_1|G), \rho(v_2|G), \dots, \rho(v_n|G)\}$, causing graph representations learned by GNNs fail to capture the similarity of input graphs when GNNs are enhanced by graph canonization. We theoretically prove that GNNs using graph canonization to generate nodes' positional encodings are unstable. Thus, there is a trade-off between the stability and expressivity in GNNs equipped with the graph canonization as an enhancer.

In the paper, we theoretically prove that the trade-off can not be generally addressed due to the individualization-refinement paradigm used in practical graph canonization tools. Consequently, we develop a notion of universal graph canonization to address the trade-off. Though the universal graph canonization problem is also NP-hard, we characterize a widely applicable sufficient condition when it is solvable through an injective (node labeling) function $\tau(G|\mathbb{G}) : V \rightarrow \mathbb{N}$, which utilizes the augmented information across the whole graph dataset $\mathbb{G} = \{G_n | n = 1, 2, \dots, N\}$ to introduce node asymmetry consistent with subgraph isomorphism in \mathbb{G} . That is, for any common subgraph G' of G_1 and G_2 in dataset \mathbb{G} , the output of $\tau(G_1|\mathbb{G})$ and $\tau(G_2|\mathbb{G})$ are *identical* on subgraph G' . Then, GNNs with nodes' positional encodings of $\{\tau(v_1|\mathbb{G}), \tau(v_2|\mathbb{G}), \dots, \tau(v_n|\mathbb{G})\}$ is proven to be stable, indicating that GNNs enhanced by the universal graph canonization can maximize the expressivity while maintaining the stability. In addition, we also show that $\tau(v|\mathbb{G})$ can be used to inject the node asymmetry in the readout layer of a GNN. Instead of applying symmetric set functions such as mean/sum, a list \mathbb{W} of trainable weight matrices is shared across graphs \mathbb{G} , and the readout layer multiplies representation of node v and the trainable parameter matrix $\mathbb{W}[\tau(v|\mathbb{G})]$ before the mean/sum operation.

The key contributions in this paper are as follows: 1) we propose a novel plug-and-play architecture to enhance GNNs by generating nodes’ positional encodings with graph canonization algorithms, and theoretically study its’ strengths and limitations. The proposed graph-canonization-enhanced GNN (GC-GNN) has the maximized expressivity in distinguishing non-isomorphic graphs, and our theory reveals the trade-off between the expressivity and model stability. 2) We theoretically solve the trade-off by introducing a notion of universal graph canonization, and propose a widely applicable sufficient condition to solve it for numerous graph datasets, including gene networks, brain networks, Bayesian networks, etc. 3) A comprehensive set of experiments demonstrates the effectiveness of proposed method. In popular graph benchmark datasets, GC-GNN successfully enhances GNNs’ performance and achieves competitive results. In graph datasets where the universal graph canonization is tractable by our sufficient condition theorem, the GNNs enhanced by the universal graph canonization (UGC-CGNN) consistently outperforms GNN baselines and improves the SOTA performance up to 31% over baselines.

1.1 OTHER RELATED WORKS

Graph canonization problem is proven to be NP-hard (Babai & Luks, 1983). Practical canonization tools such as Nauty (McKay & Piperno, 2014) and Bliss (Junttila & Kaski, 2012), are developed to effectively find the canonical form in practice. PATCHY-SAN (Niepert et al., 2016) uses graph canonization tools as a black-box function to determine the global/local node order so that CNNs can be applied to fixed-size patches extracted from nodes’ neighborhood. On the other hand, PFGNN (Dupty et al., 2021) train neural architectures with particle filtering to mimic the paradigm of individualization and refinement (McKay & Piperno, 2014; Junttila & Kaski, 2011) in practical graph canonization tools.

2 GRAPH CANONIZATION AND STABILITY OF GNNs

In this section, we introduce useful concepts. and then reveal the trade-off between the expressivity and stability in GNNs enhanced by graph canonization. Let $G = (V, E, c)$ denote a colored graph of n nodes, where $V = \{v_1, v_2, \dots, v_n\}$ is the set of nodes, $E \in V \times V$ is the set of edges, and the function $c : V \rightarrow \mathbb{N}$ associates to each node an integer color (node type). The edge information is always expressed as an adjacency matrix $A \in \{0, 1\}^{n \times n}$ such that $A_{i,j} = 1$ iff edge $(i, j) \in E$.

A *colouring* of G is a surjective function from the node set V onto a set of k integers. In this paper, We use "colouring" to denote both the image of this surjective function (i.e. set of integers). A colouring is discrete if $k = n$, then each cell (i.e. set of nodes $v \in V$ with the same image) is a singleton.

2.1 GRAPH DISTANCE AND STABLE GNNs

Let $\pi : V \rightarrow V$ be a permutation operation on the node set V . We denote by v^π the image of any node $v \in V$, then $\pi(G)$ (i.e. permutation operation on a graph G) generates another colored graph $\pi(G) = G^\pi = (V, E^\pi, c^\pi)$ such that (1) $(v_1^\pi, v_2^\pi) \in E^\pi$ iff $(v_1, v_2) \in E$ (i.e. $A_{v_1, v_2}^\pi = A_{v_1, v_2}$) and (2) $c^\pi(v^\pi) = c(v)$. Each permutation operation π associates to a n -dimension permutation matrix P^π in $\{0, 1\}^{n \times n}$, where each row and each column has only one single 1. All the permutation operation π on graphs of n nodes formulate a permutation group $\Pi(n)$.

Given two n -size graphs $G_1 = (V_1, E_1, c_1)$, $G_2 = (V_2, E_2, c_2)$ and their corresponding adjacency matrix A_1 and A_2 , there exists a permutation operation $\pi^* \in \Pi(n)$ associates to the permutation matrix P^* that best aligns the graph structures and the node colors (i.e. node features),

$$P^* = \operatorname{argmin}_{P \in \Pi} \|A_1 - PA_2P^T\|_F + \sum_i^n c_1(i)! = c_2(\pi(i))$$

The distance between two graphs is thus characterized as $d(G_1, G_2) = \|A_1 - P^*A_2P^{*T}\|_F + \sum_i c_1(i)! = c_2(\pi^*(i))$, which measures the similarity of two graphs of the same size.

Equipped with the notion of graph distance, we characterize the the stability of GNN models. The GNN model provides graph representation vector based on adjacency information and node features,

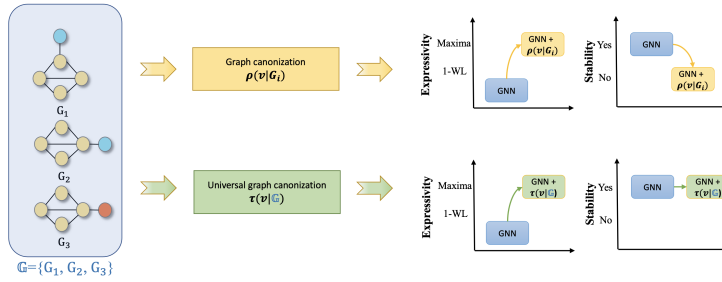


Figure 1: Overview of graph canonization techniques in the design of GNNs. Graph canonization improves the expressivity of GNNs at the cost of stability. Consequently, universal graph canonization is proposed to alleviate the problem .

then we express it as $g(A, X)$, where X is a 2-dimension tensor of one-hot features of node colors. Unless specified, following theoretical analysis assumes a GNN model consists of several message passing (MP) layers and a sum readout layer.

Definition 2.1 (Stability). A GNN model g is claimed to be stable under X , if there exists a constant $C > 0$, for any two graphs G_1, G_2 , g satisfies $\|g(A_1, X_1) - g(A_2, X_2)\|_2 \leq Cd(G_1, G_2)$.

In analog to Wang et al. (2022), the stability of a GNN model guarantees that similar graphs in the graph distance space will be mapped to similar representations in the vectorial space. Hence, it will provide good generalization ability to apply GNNs on unseen graphs. Overall, the stability and expressivity are two fundamental design principles of GNN architectures. The stability helps to bound the gap between the representations of an unseen testing graph and a similar but different training graph, while the higher expressivity enables GNNs to recognize more graph structures.

2.2 GNNs WITH GRAPH CANONIZATION

Two colored graphs G_1 and G_2 of n nodes are isomorphic (denoted by $G_1 \simeq G_2$) if there exists a permutation operation $\pi \in \Pi(n)$ such that $\pi(G_1) = G_2$. The set all colored graphs isomorphic to G forms it’s isomorphism class $ISO(G) = \{G' | G' \simeq G\}$, while an automorphism of G is an isomorphism that maps G onto itself.

Definition 2.2 (Graph canonization) Graph canonization f_n is a function that maps a colored graph to an isomorphism of the graph itself (a graph in $ISO(G)$) such that $\forall \pi \in \Pi(n), f_n(G) = f_n(\pi(G))$.

In other words, graph canonization assigns to each coloured graph an isomorphic coloured graph that is a unique representative of its isomorphism class. The order of nodes $v \in f_n(G)$ are denoted as $\rho(v|G)$. Then, the graph canonization provides a unique discrete colouring $\{\rho(v_1|G), \rho(v_2|G), \dots, \rho(v_n|G)\}$ as nodes’ positions for each isomorphism class $ISO(G)$ to break the symmetry of nodes.

Lemma 2.3 Let P be a 2-dimension tensor of one-hot features of the discrete colouring generated by an arbitrary graph canonization algorithm. A GNN model g that takes P as nodes’ positional encodings maximizes the expressivity, if graph convolution layers of g are injective.

Lemma 2.4 Let P be a 2-dimension tensor of one-hot features of the discrete colouring generated by a graph canonization algorithm follows the individualization-refinement paradigm. A GNN model g is stable under X , and is not stable under $X \oplus P$, where \oplus denotes the concatenation operation.

We prove lemma 2.3 and lemma 2.4 in Appendix C. Graph canonization algorithms that follow the individualization-refinement paradigm Grohe et al. (2017) will respect the order of initial node colors/types when breaking ties to introduce the node asymmetry, thus there always exists similar graphs to have complete different discrete colourings as Figure 2 illustrates. These two lemmas indicate the trade-off of expressivity and stability in GNNs enhanced by graph canonization. Then, graph-canonization-enhanced GNNs (GC-GNNs) can distinguish more graph structures in the training data, yet the ability of generalizing well to unseen testing data is deteriorated to some extent. Hence, we study how to overcome this trade-off in next section. Furthermore, since the graph canonization

problem is NP-hard, and practical tools like Nauty (McKay & Piperno, 2014) and Bliss (Junttila & Kaski, 2012) for the problem always follow the individualization-refinement paradigm, the trade-off is not generally solvable in practice.

3 UNIVERSAL GRAPH CANONIZATION

In this section, we first introduce the notion of universal graph canonization, and theoretically prove that it can maximize GNNs’ expressive power without losing the stability. Then we propose a widely applicable sufficient condition to apply GNNs with universal graph canonization in numerous graphs.

3.1 UNIVERSAL GRAPH CANONIZATION

Ideally, the maximally powerful GNNs are expected to be expressive and stable. Thus, our goal is to generate a discrete colouring $\{\tau(v_1), \tau(v_2), \dots, \tau(v_n)\}$ that is equivalent to the output colouring $\{\rho(v_1|G), \rho(v_2|G), \dots, \rho(v_n|G)\}$ of a general graph canonization algorithm in breaking the node symmetry, while maintaining the stability to provide better generalization performance.

Definition 3.1 (*Universal graph canonization*) Let $\mathbb{G} = \{G_i | i = 1, 2, \dots, N\}$ be a graph dataset. A discrete colouring function $\tau(v|\mathbb{G}) : V \rightarrow \mathbb{N}$ is claimed as an universal graph canonization for \mathbb{G} , if \forall common subgraph G' of $G_1, G_2 \in \mathbb{G}$. $\tau(G_1|\mathbb{G})$ and $\tau(G_2|\mathbb{G})$ are identical in G' .

It is straightforward that the output discrete colouring $\{\tau(v_1|\mathbb{G}), \tau(v_2|\mathbb{G}) \dots \tau(v_n|\mathbb{G})\}$ of the proposed universal graph canonization is equivalent to $\{\rho(v_1|G), \rho(v_2|G), \dots, \rho(v_n|G)\}$ of a general graph canonization algorithm in breaking nodes’ symmetry and distinguishing non-isomorphic graphs. Both of them will be same for isomorphic graphs and be different for non-isomorphic graphs. In fact, one can get the canonical form of an input graph G by sorting nodes according to the discrete colouring $\{\tau(v_1|\mathbb{G}), \tau(v_2|\mathbb{G}) \dots \tau(v_n|\mathbb{G})\}$.

The main difference between the output discrete colourings $\{\tau(v_1|\mathbb{G}), \tau(v_2|\mathbb{G}) \dots \tau(v_n|\mathbb{G})\}$ and $\{\rho(v_1|G), \rho(v_2|G), \dots, \rho(v_n|G)\}$ lies in their resistance ability to graph perturbations. The graph canonization tools employ the technique of individualization-refinement to sequentially refine a colouring until it is discrete. Then, the output discrete colouring $\{\rho(v_1|G), \rho(v_2|G), \dots, \rho(v_n|G)\}$ is heavily dependent on the order of nodes to individualize, which is determined by the symmetry in the graph structure. Consequently, even a small perturbation that breaks the symmetry, such as recoloring a single node, may causes a significant change of the sequence of individualized nodes, resulting in a complete different output colouring. That is, the change of output colouring happens across all nodes regardless of their geometric relation to the position of the perturbed node. Figure 2 provides an example as the illustration. After we recolor the top yellow node as orange (i.e. $G_1 \rightarrow G_2$), the output discrete colouring (i.e. numbers on nodes) of left triangle and bottom triangle are completely different, yet these subgraphs are isomorphic in G_1 and G_2 . In contrast, the universal graph canonization generate the discrete colouring conditioned on whole graph dataset \mathbb{G} to guarantee the color consistency among subgraphs G' of any pair of graphs in \mathbb{G} . Thus, the graph perturbation to nodes/edges outside G' will not affects generated colours within G' .

Theorem 3.2 Let $\tau(v|\mathbb{G})$ be an universal graph canonization for dataset \mathbb{G} , and T be the 2-dimensional tensor of one-hot features of discrete colouring $\{\tau(v_1|\mathbb{G}), \tau(v_2|\mathbb{G}) \dots \tau(v_n|\mathbb{G})\}$. A GNN model g under $X \oplus T$ is stable, where \oplus denotes the concatenation operation.

We prove Theorem 3.2 in Appendix D. This theory guarantees that GNNs enhanced by universal graph canonization (UGC-GNNs) are stable. In addition, since universal graph canonization is equally powerful as the general graph canonization in distinguishing non-isomorphic graphs, UGC-GNNs can also maximize the expressive power in graph discrimination.

3.2 A SUFFICIENT CONDITION FOR GNNs WITH UNIVERSAL GRAPH CANONIZATION

Having recognized the stability and expressivity of UGC-GNN, we next discuss its’ applicability in real-world graph representation learning. The main challenge is to effectively solve the universal graph canonization problem on a given dataset \mathbb{G} . Unlike the general graph canonization problem

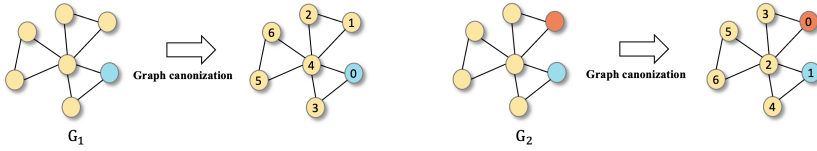


Figure 2: Illustration of the limitation in graph canonization follows the individualization-refinement paradigm. In the example, initial node colors/types follow the order: orange < blue < yellow. Then, two similar graphs G_1 and G_2 will always have complete different discrete colouring generated by graph canonization algorithms.

where many practical tools, such as Nauty (McKay & Piperno, 2014) and Bliss (Junttila & Kaski, 2012), are developed to effectively implement the algorithm, there is no existing software to solve the universal graph canonization problem. Furthermore, according to the definition 3.1, this problem is at least as hard as the subgraph isomorphism problem, thereby is NP-hard.

Lemma 3.3 *Let $l(v|\mathbb{G}) : V \rightarrow \mathbb{N}$ be an injective function. $l(v|\mathbb{G})$ is a universal graph canonization, if for $\forall v_1, u_1 \in G_1, v_2, u_2 \in G_2, G_1, G_2 \in \mathbb{G}$ such that $l(v_1|\mathbb{G}) = l(v_2|\mathbb{G})$ and $l(u_1|\mathbb{G}) = l(u_2|\mathbb{G})$, we have $(v_1, u_1) \in E_1 \leftrightarrow (v_2, u_2) \in E_2$, where \leftrightarrow is an equivalence relation.*

We prove Lemma 3.3 in Appendix E. To explain a bit, this lemma provides a sufficient condition to compute the discrete coloring $\{\tau(v_1|\mathbb{G}), \tau(v_2|\mathbb{G}) \dots \tau(v_n|\mathbb{G})\}$. For a graph learning problem in real world, once a function $l(v|\mathbb{G})$ that satisfies conditions in lemma 3.3 is tractable, we can use it to find the universal graph canonization for UGC-GNN.

Application scenarios We prove Lemma 3.3 in Appendix E, and this lemma provides a sufficient condition to compute the universal graph canonization. Together with the definition 3.1, universal graph canonization is tractable in numerous scenarios: (1) In gene networks Shuhendler et al. (2010); Dong et al. (2023), each gene appears at most once in each gene network, and the connection of any pair of genes is shared among different gene networks, then $l(v|\mathbb{G})$ can be extracted by lexicographically sorting all genes appear in the dataset; (2) In brain graphs Li et al. (2021); Venkataraman et al. (2016), the brain fMRI images are parcellated into ROIs (regions of interests) as nodes, and edges are computed by the functional correlation matrix between ROIs. Since these ROIs can be pre-ordered across all brain images, these pre-orders can be used as the output of the $l(v|\mathbb{G})$. (3) In traffic networks such as METR-LA and Roadnet-CA Li et al. (2017), nodes represent fixed intersections or road endpoints whose pre-defined orders can be treated as the output of $l(v|\mathbb{G})$. (4) Many well-known computer vision datasets such as MNIST and CIFAR10 are also transformed to graph signals on fixed-grid-like structures, where $l(v|\mathbb{G})$ can be defined by lexicographically sorting nodes' grid positions, and these datasets have become benchmarks for graph learning recently Dwivedi et al. (2020); (5) In many DAG learning problems Zhang et al. (2019), such as neural architecture search (NA) and Bayesian structure learning (BN), the function $l(v|\mathbb{G})$ can be obtained by sorting nodes according to their positions in the Hamiltonian path in NA or to their node types in BN.

Readout layer Both message passing layers and readout layers contribute to GNN's learning ability in the graph-level prediction. Thus, UGC-GNN also propose to incorporate the discrete coloring $\{l(v_1|\mathbb{G}), l(v_2|\mathbb{G}) \dots l(v_n|\mathbb{G})\}$ in the readout layer to break nodes' symmetry. Specifically, a weighted summation over set of node representation $\{h_v^T | v \in V\}$ is used, where the trainable weight matrices are associated w.r.t the discrete colouring $\{l(v_1|\mathbb{G}), l(v_2|\mathbb{G}) \dots l(v_n|\mathbb{G})\}$,

$$\text{Readout}(\{h_v^T | v \in V\}) = \sum_{v \in V} W_{l(v|\mathbb{G})} h_v^T$$

Here, h_v^T is the output representation of node v in the last (T -th) message passing layer of UGC-GNN. Thus, UGC-GNN introduces node asymmetry in both graph convolution layers and readout layer.

Lemma 3.4 *UGC-GNN is permutation invariant.*

We prove Lemma 3.4 in Appendix F. As nodes in a graph have no intrinsic ordering, GNN model should also be permutation invariant to the permutation operations. That is, $\forall P \in \Pi(n)$, we have $g(A, X) = g(PAP^T, AX)$. Machine learning model fail to do so will lead to a waste of training

data and computation time. Hence, the proposed UGC-GNN is stable, maximally expressive, and permutation-invariant.

4 EXPERIMENTS

In this section, we evaluate the effectiveness of proposed graph-canonization-enhanced GNNs against competitive GNN baselines. Concretely, we first conduct experiments on synthetic datasets and TU datasets to test the general performance of proposed method (GC-GNN). Then we demonstrate the superiority of our UGC-GNN when universal graph canonization is solvable through proposed sufficient condition, and use challenging gene network datasets, brain graph dataset, DAG datasets as the benchmark in this scenario. Details of datasets are provided in Appendix A.

4.1 DATASETS

Synthetic datasets EXP (Abboud et al., 2020) and CSL (Murphy et al., 2019) are two graph isomorphism test datasets where non-isomorphic regular graphs are required to be distinguished. Specifically, the EXP dataset contains 600 pairs of 1-WL-indistinguishable but non-isomorphic graphs, while the CSL dataset contains 150 4-regular graphs from 10 isomorphism groups.

TU datasets TU datasets (Dobson & Doig, 2003; Toivonen et al., 2003) include five graph datasets: PROTEINS, PTC-MR, MUTAG, ENZYMES, D&D. TU datasets are widely used to perform the graph classification task.

Gene network datasets Gene networks are ubiquitous in bioinformatics. In the experiment, we select three gene network datasets: RosMap, Mayo, and Cancer, for the challenging graph classification tasks in bioinformatics. Mayo and RosMap are designed for the Alzheimer’s disease (AD) classification (De Jager et al., 2018; Allen et al., 2016); Cancer is designed for the cancer subtype classification. In gene networks, gene expressions are used as node features, while edges between genes are collected from KEGG (Kyoto Encyclopedia of Genes and Genomes) Kanehisa & Goto (2000) based on the physical signaling interactions from documented medical experiments.

Brain graph datasets Brain graphs in the public dataset fMRI ABIDE Di Martino et al. (2014) take as nodes the ROIs (regions of interests) parcellated from brain fMRI images, and use the computed functional correlation matrix between ROIs as edges. The objective is to classify the brain state.

DAG datasets This experiment contains two DAG datasets: NA and BN. In dataset NA, neural architectures generated by the software ENAS (Pham et al., 2018), and the corresponding weight-sharing (WS) accuracy on CIFAR-10 (Krizhevsky et al., 2009) is pre-computed for each architecture. In dataset BN, Bayesian networks (DAGs) are randomly sampled by the `bnlearn` package (Scutari, 2010). Each DAG is associated with a Bayesian Information Criterion (BIC) score that measures the architecture performance on dataset Asia (Lauritzen & Spiegelhalter, 1988).

4.2 BASELINES AND EXPERIMENT CONFIGURATION

The experiment takes three types of baselines: (1) popular GNNs and graph Transformers that achieve top places on OGB leaderboard: GCN (Kipf & Welling, 2016), GIN (Xu et al., 2019), GAT (Velickovic et al., 2018), GraphSAGE (Hamilton et al., 2017), SAN (Kreuzer et al., 2021), Graphormer (Ying et al., 2021); (2) Expressive GNNs beyond 1-WL: NGNN (Zhang & Li, 2021), GCN-RNI (Abboud et al., 2020), PNA (Corso et al., 2020), GINE (Brossard et al., 2020), PPGN (Maron et al., 2019), GraphSNN (Wijesinghe & Wang, 2022) and GNN-AK+ (Zhao et al., 2021); SignNet (Lim et al., 2022), ESAN (Bevilacqua et al., 2021), DropGNN (Papp et al., 2021); (3) Dominant DAG GNNs: GraphRNN (You et al., 2018), S-VAE (Bowman et al., 2016), D-VAE (Zhang et al., 2019), DAGNN(Thost & Chen, 2021).

Gene networks have received considerable attention in bioinformatics and numerous deep learning (DL) models are developed recently to analyze gene networks. Thus, beside above GNN baselines, we also compare our UGC-GNN against powerful DL models in bioinformatics: TransSynergy Liu & Xie (2021), SANepool Dong et al. (2023), Decagon Zitnik et al. (2018), DimiG Pan & Shen (2019), MLA-GNN Xing et al. (2022). We thoroughly introduce graph-structured data in bioinformatics and their DL baselines in Appendix H to explain why we select above DL models as additional baselines.

We perform 10-fold (or 5-fold) cross validation for robust comparison. All experiments are implemented in the environment of PyTorch using NVIDIA A40 GPUs. Our graph-canonization-based GNNs take backbone GNNs from $\{GIN, GCN, GraphSAGE, GAT\}$. In GNN baselines, the embedding dimension of graph convolution layer is set to be 32. The number of graph convolution layer is selected from the set $\{2, 3, 4\}$. The graph-level readout function is selected from $\{mean, sum, sortpool\}$. In NGNN, we use height-1 rooted subgraphs to avoid the out-of-memory problem in gene network datasets. The experimental settings follow Dong et al. (2022b) on dataset NA/BN and follow Zhang & Li (2021) on TU datasets. The training protocols is composed of the selection of the evaluation rates and training stop rules. Specifically, the learning rate of optimizer picks the best from the set $\{1e-4, 1e-3, 1e-2\}$; the training process is stopped when the validation metric does not improve further under a patience of 10 epochs.

4.3 EVALUATION OF GC-GNN

To test the general performance of GNNs enhanced by graph canonization (i.e. GC-GNN), we conduct experiments to answer following questions:

Q1: Can GC-GNN empirically achieve the maximal expressive power in distinguishing non-isomorphic graphs?

Q2: To what extent can GC-GNN improve the predictive performance without ameliorating the model stability?

Answer to Q1 (Table 1) Here we start with the first question. In this experiment, we test the expressive power of GC-GNN on two synthetic datasets, EXP and CSL. use GIN and GCN as backbone GNN. As Table 1 shown, for any backbone GNN, GC-GNN can significantly improve the expressive power and distinguishes almost all the 1-WL indistinguishable graphs.

Model	EXP		CSL	
	Train Accuracy \uparrow	Test Accuracy \uparrow	Train Accuracy \uparrow	Test Accuracy \uparrow
GCN (backbone)	0.5000 \pm 0.000	0.5000 \pm 0.000	0.1213 \pm 0.0034	0.0133 \pm 0.0281
GC-GNN (GCN)	0.9918 \pm 0.0102	0.9267 \pm 0.0858	0.9994 \pm 0.0008	0.9583 \pm 0.0791
GIN (backbone)	0.5000 \pm 0.000	0.5000 \pm 0.000	0.1400 \pm 0.0663	0.1157 \pm 0.0081
GC-GNN (GIN)	1.00 \pm 0.00	0.9975 \pm 0.0056	1.00 \pm 0.00	0.9667 \pm 0.0720

Table 1: Evaluation of expressive power on synthetic datasets for graph isomorphism test.

Answer to Q2 (Table 2) Lemma 2.4 demonstrates the limitation of GC-GNN. This experiment empirically show that GC-GNN can still achieve impressive performance when the stability concern is not well addressed. The widely adopted TU datasets are used as the example, and Table 2 presents the results. 1) GC-GNN consistently brings performance gains to GNN backbones by a large margin, and the erformance gain is up to 29.6% 2) Nested GNN has been shown to a powerful plug-and-play framework to improve GNNs’ expressivity beyond 1-WL. Compared to this popular subgraph-based GNN, GC-GNN also provides a considerable performance improvement without the additional space/computation cost raised by the subgraph extraction. 3) Compared to recent powerful GNNs like GraphSNN, GNN-AK+, SignNet, ESAN, etc, GC-GNN can still achieve highly competitive performance. For instance, GC-GNN significantly improves the state-of-the-art performance on $D\&D$ to an accuracy above 90%.

4.4 EVALUATION OF UGC-GNN

Though we have shown the huge potential of GC-GNN in enhancing GNNs, the loss of model stability still raises challenges when applied to some graph datasets, especially these with large-scale graphs. For instance, gene networks in datasets Mayo, Rosmap and Cancer contain more than 3000 nodes, then Table 3 shows that GC-GNN with a backbone of GIN even performs worsen than GIN. More similar ablation results are available in Appendix G. Another example is the experiments on OGB datasets. Appendix B shows that GC-GNN can improve base GNNs on OGB datasets (ogbg-molhiv, ogbg-molpcba) to a close performance to ESAN with ED policy, yet they are not comparable to the SOTA performance. These results empirically demonstrate the importance of maintaining GNN’s stability and the necessity of designing UGC-GNN.

	D&D ↑	MUTAG ↑	PROTEINS ↑	PTC-MR ↑	ENZYMES ↑
GCN (backbone)	71.6 ± 2.8	73.4 ± 10.8	71.7 ± 4.7	56.4 ± 7.1	27.3 ± 5.5
GraphSAGE (backbone)	71.6 ± 3.0	74.0 ± 8.8	71.2 ± 5.2	57.0 ± 5.5	30.7 ± 6.3
GIN (backbone)	70.5 ± 3.6	84.5 ± 8.9	70.6 ± 4.3	51.2 ± 9.2	38.3 ± 6.4
GAT (backbone)	71.0 ± 4.4	73.9 ± 10.7	72.0 ± 3.3	57.0 ± 7.3	30.2 ± 4.2
Nested GCN	76.3 ± 3.8	82.9 ± 11.1	73.3 ± 4.0	57.3 ± 7.7	31.2 ± 6.7
Nested GraphSAGE	77.4 ± 4.2	83.9 ± 10.7	74.2 ± 3.7	57.0 ± 5.9	30.7 ± 6.3
Nested GIN	77.8 ± 3.9	87.9 ± 8.2	73.9 ± 5.1	54.1 ± 7.7	29.0 ± 8.0
Nested GAT	76.0 ± 4.4	81.9 ± 10.2	73.7 ± 4.8	56.7 ± 8.1	29.5 ± 5.7
GraphSNN	79.6 ± 2.9	87.8 ± 7.6	74.7 ± 3.9	54.6 ± 8.5	36.8 ± 5.1
GIN-AK+	80.3 ± 3.1	88.5 ± 8.6	75.2 ± 4.7	55.1 ± 9.2	38.5 ± 6.3
SignNet	78.2 ± 4.1	88.3 ± 9.2	75.6 ± 4.1	64.3 ± 7.1	37.5 ± 6.4
GNN-RNI	75.8 ± 3.0	90.4 ± 7.4	73.5 ± 4.5	58.2 ± 6.3	30.7 ± 5.6
ESAN	79.7 ± 3.8	91.0 ± 4.8	75.8 ± 4.5	65.7 ± 7.0	37.9 ± 6.3
DropGNN	78.5 ± 6.0	90.4 ± 7.0	76.3 ± 6.1	62.7 ± 8.4	38.3 ± 7.1
GC-GNN (GCN)	91.3 ± 9.7	86.2 ± 9.9	76.7 ± 5.1	66.9 ± 7.1	37.7 ± 6.9
GC-GNN (GraphSAGE)	92.1 ± 8.1	89.4 ± 8.8	75.8 ± 4.0	62.5 ± 5.1	35.7 ± 5.9
GC-GNN (GIN)	91.4 ± 8.6	86.2 ± 6.7	74.4 ± 3.7	57.2 ± 7.5	30.7 ± 4.9
GC-GNN (GAT)	90.5 ± 9.0	87.3 ± 7.5	75.6 ± 3.8	62.2 ± 7.0	32.0 ± 5.8
Ave. improvement over backbone	28.2%	14.6%	6.0%	12.3%	8.9%
Max. improvement over backbone	29.6%	20.8%	7.0%	18.6%	38.1%
Ave. improvement over Nested GNN	18.7%	3.8%	2.5%	10.5%	12.9%
Max. improvement over Nested GNN	19.7%	6.6%	4.6%	16.8%	20.8%

Table 2: Prediction accuracy (%) on TU datasets. Highlighted are the **best** results.

Methods	Mayo		RosMap		Cancer		fMRI-ABIDE	
	Accuracy ↑	F1 score ↑	Accuracy ↑	F1 score ↑	Accuracy ↑	F1 score ↑	Accuracy ↑	F1 score ↑
GIN	0.496 ± 0.042	0.484 ± 0.036	0.471 ± 0.039	0.482 ± 0.041	0.537 ± 0.045	0.512 ± 0.047	0.592 ± 0.035	0.553 ± 0.046
GCN	0.561 ± 0.049	0.535 ± 0.021	0.520 ± 0.036	0.571 ± 0.032	0.593 ± 0.039	0.561 ± 0.042	0.607 ± 0.031	0.566 ± 0.062
GraphSAGE	0.503 ± 0.031	0.471 ± 0.021	0.517 ± 0.038	0.462 ± 0.026	0.482 ± 0.048	0.512 ± 0.051	0.623 ± 0.057	0.596 ± 0.070
GAT	0.515 ± 0.034	0.547 ± 0.021	0.491 ± 0.037	0.508 ± 0.042	0.461 ± 0.039	0.532 ± 0.031	0.614 ± 0.034	0.590 ± 0.052
GSN	0.536 ± 0.018	0.551 ± 0.021	0.551 ± 0.024	0.516 ± 0.020	0.576 ± 0.037	0.602 ± 0.041	0.616 ± 0.019	0.593 ± 0.047
PNA	0.551 ± 0.037	0.579 ± 0.046	0.560 ± 0.035	0.584 ± 0.041	0.620 ± 0.029	0.691 ± 0.033	0.613 ± 0.071	0.585 ± 0.072
GINE	0.539 ± 0.041	0.571 ± 0.038	0.572 ± 0.050	0.583 ± 0.046	0.629 ± 0.044	0.619 ± 0.058	0.620 ± 0.029	0.592 ± 0.061
NGNN	0.517 ± 0.033	0.504 ± 0.031	0.509 ± 0.030	0.481 ± 0.042	0.516 ± 0.049	0.532 ± 0.056	0.621 ± 0.051	0.557 ± 0.085
PPGN	0.522 ± 0.021	0.510 ± 0.037	0.539 ± 0.033	0.607 ± 0.031	0.499 ± 0.025	0.484 ± 0.042	0.633 ± 0.042	0.600 ± 0.053
GCN-RNI	0.513 ± 0.027	0.501 ± 0.031	0.496 ± 0.041	0.512 ± 0.037	0.521 ± 0.041	0.502 ± 0.069	0.624 ± 0.021	0.598 ± 0.050
SignNet	0.527 ± 0.035	0.514 ± 0.029	0.544 ± 0.030	0.609 ± 0.037	0.572 ± 0.044	0.553 ± 0.048	0.628 ± 0.041	0.597 ± 0.052
ESAN	0.579 ± 0.035	0.605 ± 0.037	0.581 ± 0.042	0.614 ± 0.040	OOM	OOM	0.629 ± 0.058	0.596 ± 0.061
DropGNN	0.533 ± 0.042	0.517 ± 0.039	0.557 ± 0.045	0.571 ± 0.050	OOM	OOM	0.619 ± 0.063	0.593 ± 0.072
GC-GNN (GIN)	0.483 ± 0.026	0.472 ± 0.031	0.486 ± 0.041	0.510 ± 0.037	0.539 ± 0.041	0.532 ± 0.069	0.610 ± 0.033	0.572 ± 0.056
UGC-GNN (GIN)	0.624 ± 0.036	0.713 ± 0.022	0.701 ± 0.025	0.689 ± 0.019	0.714 ± 0.011	0.701 ± 0.032	0.648 ± 0.033	0.625 ± 0.060

Table 3: Experimental results on bioinformatical tasks: gene network datasets and brain graph datasets. Shown is the mean ± s.d. of 10 runs with different random seeds. **Best results** are highlighted.

The superior representation learning ability. Table 3 and Table 4 This experiment evaluates UGC-GNN against powerful and popular GNN baselines on many real-world datasets where Lemma 3.3 can help to find the universal graph canonization. Table 3 and Table 4 show that UGC-GNN consistently achieves the state-of-the-art (SOTA) performance and can provide a performance improvement up to 31% over GNN baselines. The observation aligns well with our theorem 3.2. Overall, the superior representation learning ability of UGC-GNN comes from its’ ability to maximize the expressivity in distinguishing graph structures while maintaining the stability.

Efficiency. Another significant advantage of enhancing GNNs with universal graph canonization is the time/space complexity. Suppose the graph has n nodes with a maximum degree d , then UGC-GNN has a space complexity of $\mathcal{O}(n)$ and each layer takes $\mathcal{O}(nd)$ operations. In contrast, high-order GNNs like PPGN has a space complexity of $\mathcal{O}(n^2)$ for each layer and a $\mathcal{O}(n^3)$ time complexity; Subgraph-based GNNs (to radius r) has a $\mathcal{O}(nd^r)$ space complexity and each layer takes $\mathcal{O}(nd^{r+1})$ operations. In many real-world tasks especially in bioinformatics, graphs has a large n and r , which makes existing dominant expressive GNNs (high-order GNNs and subgraph-based GNNs) unsuitable. Table 3 indicates that existing dominant expressive GNNs can easily have the our-of-memory (OOM) problem (like ESAN and DropGNN), while Appendix I shows that UGC-GNN can significantly reduce the computation time. Specially, UGC-GNN only requires about $\frac{1}{4}$ and $\frac{1}{10}$ average time per epoch compared to subgraph-based GNN (NGNN) and high-order GNN (PPGN), respectively.

The optimal solution to the challenging gene network analysis. Table 5. Gene networks are the prevailing data structure in Bioinformatics (Podolsky & Greene, 2011; Carew et al., 2008). Recent years, it has emerged as a popular topic of developing the de facto standard for effective representation learning methods over gene networks, which leads to potential advancements in clinical applications including drug synergy prediction (Hopkins, 2008; Podolsky & Greene, 2011), Alzheimer’s disease (AD) detection (Song et al., 2019; Qin et al., 2022) and cancer subtype classification (Lu & Han, 2003). In the experiment, we compare UGC-GNN against existing SOTA deep learning (DL) models

Methods	NA		BN	
	RMSE ↓	Pearson's r ↑	RMSE ↓	Pearson's r ↑
GCN	0.832 ± 0.001	0.527 ± 0.001	0.599 ± 0.006	0.809 ± 0.002
DAGNN	0.264 ± 0.004	0.964 ± 0.001	0.122 ± 0.004	0.991 ± 0.000
D-VAE	0.384 ± 0.002	0.920 ± 0.001	0.281 ± 0.004	0.964 ± 0.001
S-VAE	0.478 ± 0.002	0.873 ± 0.001	0.499 ± 0.006	0.873 ± 0.002
GraphRNN	0.726 ± 0.002	0.669 ± 0.001	0.779 ± 0.007	0.634 ± 0.001
DeepGMG	0.478 ± 0.002	0.873 ± 0.001	0.843 ± 0.007	0.555 ± 0.003
Graphormer	0.352 ± 0.002	0.936 ± 0.001	0.181 ± 0.004	0.971 ± 0.001
SAN	0.311 ± 0.003	0.950 ± 0.001	0.158 ± 0.005	0.989 ± 0.001
UGC-GNN (GIN)	0.253 ± 0.002	0.964 ± 0.001	0.120 ± 0.004	0.992 ± 0.001

Table 4: Experimental results on DAG datasets. **Best results** are highlighted.

for gene network analysis. Table 5 indicates that UGC-GNN outperforms these DL models and is the optimal solution to the challenging gene network analysis.

Methods	Mayo		RosMap		Cancer	
	Accuracy ↑	F1 score ↑	Accuracy ↑	F1 score ↑	Accuracy ↑	F1 score ↑
SANepool	0.501 ± 0.041	0.486 ± 0.036	0.492 ± 0.036	0.507 ± 0.040	0.511 ± 0.032	0.508 ± 0.047
Decagon	0.561 ± 0.049	0.535 ± 0.021	0.520 ± 0.036	0.571 ± 0.032	0.593 ± 0.039	0.561 ± 0.042
DimiG	0.561 ± 0.049	0.535 ± 0.021	0.520 ± 0.036	0.571 ± 0.032	0.593 ± 0.039	0.561 ± 0.042
TransSynergy	0.532 ± 0.019	0.547 ± 0.028	0.540 ± 0.025	0.558 ± 0.032	0.588 ± 0.029	0.544 ± 0.035
MLA-GNN	0.589 ± 0.033	0.614 ± 0.036	0.595 ± 0.028	0.622 ± 0.040	0.631 ± 0.035	0.640 ± 0.037
UGC-GNN (GIN)	0.624 ± 0.036	0.713 ± 0.022	0.701 ± 0.025	0.689 ± 0.019	0.714 ± 0.011	0.701 ± 0.032

Table 5: Comparison to powerful DL baselines in Bioinformatics. Shown is the mean ± s.d. of 5 runs with different random seeds. **Best results** are highlighted.

5 CONCLUSION AND DISCUSSIONS

In this paper, we propose to enhance GNNs through graph canonization that generates discrete colouring of nodes as their positional encodings to introduce node asymmetry. We theoretically show that graph-canonization-enhanced GNNs (i.e. GC-GNNs) maximize the expressivity in distinguishing non-isomorphic graphs at the cost of model stability, and then design a universal graph canonization to ameliorate this trade-off under a widely applicable sufficient condition that is satisfied in numerous real-world graph datasets. Massive experiments demonstrate the capability and great potential of GC-GNN in general graph representation learning; Furthermore, GNNs enhanced by the universal graph canonization (i.e. UGC-GNNs) show superior predictive ability and consistently achieve the state-of-the-art performance when the sufficient condition is satisfied, providing the optimal solution to many real-world applications like the challenging gene network representation learning in bioinformatics.

REFERENCES

- Ralph Abboud, Ismail Ilkan Ceylan, Martin Grohe, and Thomas Lukasiewicz. The surprising power of graph neural networks with random node initialization. *arXiv preprint arXiv:2010.01179*, 2020.
- Mariet Allen, Minerva M Carrasquillo, Cory Funk, Benjamin D Heavner, Fanggeng Zou, Curtis S Younkin, Jeremy D Burgess, High-Seng Chai, Julia Crook, James A Eddy, et al. Human whole genome genotype and transcriptome data for alzheimer’s and other neurodegenerative diseases. *Scientific data*, 3(1):1–10, 2016.
- László Babai and Eugene M Luks. Canonical labeling of graphs. In *Proceedings of the fifteenth annual ACM symposium on Theory of computing*, pp. 171–183, 1983.
- Peter L Bartlett, Dylan J Foster, and Matus J Telgarsky. Spectrally-normalized margin bounds for neural networks. *Advances in neural information processing systems*, 30, 2017.
- Beatrice Bevilacqua, Fabrizio Frasca, Derek Lim, Balasubramaniam Srinivasan, Chen Cai, Gopinath Balamurugan, Michael M Bronstein, and Haggai Maron. Equivariant subgraph aggregation networks. *arXiv preprint arXiv:2110.02910*, 2021.
- Samuel Bowman, Luke Vilnis, Oriol Vinyals, Andrew Dai, Rafal Jozefowicz, and Samy Bengio. Generating sentences from a continuous space. In *Proceedings of The 20th SIGNLL Conference on Computational Natural Language Learning*, pp. 10–21, 2016.
- Rémy Brossard, Oriol Frigo, and David Dehaene. Graph convolutions that can finally model local structure. *arXiv preprint arXiv:2011.15069*, 2020.
- Jennifer S Carew, Francis J Giles, and Steffan T Nawrocki. Histone deacetylase inhibitors: mechanisms of cell death and promise in combination cancer therapy. *Cancer letters*, 269(1):7–17, 2008.
- Gabriele Corso, Luca Cavalleri, Dominique Beaini, Pietro Liò, and Petar Veličković. Principal neighbourhood aggregation for graph nets. *Advances in Neural Information Processing Systems*, 33:13260–13271, 2020.
- Philip L De Jager, Yiyi Ma, Cristin McCabe, Jishu Xu, Badri N Vardarajan, Daniel Felsky, Hans-Ulrich Klein, Charles C White, Mette A Peters, Ben Lodgson, et al. A multi-omic atlas of the human frontal cortex for aging and alzheimer’s disease research. *Scientific data*, 5(1):1–13, 2018.
- Adriana Di Martino, Chao-Gan Yan, Qingyang Li, Erin Denio, Francisco X Castellanos, Kaat Alaerts, Jeffrey S Anderson, Michal Assaf, Susan Y Bookheimer, Mirella Dapretto, et al. The autism brain imaging data exchange: towards a large-scale evaluation of the intrinsic brain architecture in autism. *Molecular psychiatry*, 19(6):659–667, 2014.
- Paul D Dobson and Andrew J Doig. Distinguishing enzyme structures from non-enzymes without alignments. *Journal of molecular biology*, 330(4):771–783, 2003.
- Zehao Dong, Weidong Cao, Muhan Zhang, Dacheng Tao, Yixin Chen, and Xuan Zhang. Cktgnn: Circuit graph neural network for electronic design automation. In *The Eleventh International Conference on Learning Representations*, 2022a.
- Zehao Dong, Muhan Zhang, Fuhai Li, and Yixin Chen. Pace: A parallelizable computation encoder for directed acyclic graphs. *arXiv preprint arXiv:2203.10304*, 2022b.
- Zehao Dong, Heming Zhang, Yixin Chen, Philip RO Payne, and Fuhai Li. Interpreting the mechanism of synergism for drug combinations using attention-based hierarchical graph pooling. *Cancers*, 15(17):4210, 2023.
- Mohammed Haroon Dupty, Yanfei Dong, and Wee Sun Lee. Pf-gnn: Differentiable particle filtering based approximation of universal graph representations. In *International Conference on Learning Representations*, 2021.

- David Duvenaud, Dougal Maclaurin, Jorge Aguilera-Iparraguirre, Rafael Gómez-Bombarelli, Timothy Hirzel, Alán Aspuru-Guzik, and Ryan P Adams. Convolutional networks on graphs for learning molecular fingerprints. *Advances in Neural Information Processing Systems*, 2015:2224–2232, 2015.
- Vijay Prakash Dwivedi, Chaitanya K Joshi, Thomas Laurent, Yoshua Bengio, and Xavier Bresson. Benchmarking graph neural networks. *arXiv preprint arXiv:2003.00982*, 2020.
- Alex M Fout. *Protein interface prediction using graph convolutional networks*. PhD thesis, Colorado State University, 2017.
- Justin Gilmer, Samuel S Schoenholz, Patrick F Riley, Oriol Vinyals, and George E Dahl. Neural message passing for quantum chemistry. In *International Conference on Machine Learning*, pp. 1263–1272. PMLR, 2017.
- Martin Grohe. The logic of graph neural networks. In *2021 36th Annual ACM/IEEE Symposium on Logic in Computer Science (LICS)*, pp. 1–17. IEEE, 2021.
- Martin Grohe, Kristian Kersting, Martin Mladenov, and Pascal Schweitzer. Color refinement and its applications. *Van den Broeck, G.; Kersting, K.; Natarajan, S*, 30, 2017.
- Will Hamilton, Zhitao Ying, and Jure Leskovec. Inductive representation learning on large graphs. In I. Guyon, U. V. Luxburg, S. Bengio, H. Wallach, R. Fergus, S. Vishwanathan, and R. Garnett (eds.), *Advances in Neural Information Processing Systems*, volume 30. Curran Associates, Inc., 2017. URL <https://proceedings.neurips.cc/paper/2017/file/5dd9db5e033da9c6fb5ba83c7a7ebea9-Paper.pdf>.
- Moritz Hardt, Ben Recht, and Yoram Singer. Train faster, generalize better: Stability of stochastic gradient descent. In *International conference on machine learning*, pp. 1225–1234. PMLR, 2016.
- Andrew L Hopkins. Network pharmacology: the next paradigm in drug discovery. *Nature chemical biology*, 4(11):682–690, 2008.
- Weihua Hu, Matthias Fey, Marinka Zitnik, Yuxiao Dong, Hongyu Ren, Bowen Liu, Michele Catasta, and Jure Leskovec. Open graph benchmark: Datasets for machine learning on graphs. *arXiv preprint arXiv:2005.00687*, 2020.
- Tommi Junttila and Petteri Kaski. Conflict propagation and component recursion for canonical labeling. In *Theory and Practice of Algorithms in (Computer) Systems: First International ICST Conference, TAPAS 2011, Rome, Italy, April 18-20, 2011. Proceedings*, pp. 151–162. Springer, 2011.
- Tommi Junttila and Petteri Kaski. bliss: A tool for computing automorphism groups and canonical labelings of graphs. URL <http://www.tcs.hut.fi/Software/bliss>, 2012.
- Minoru Kanehisa and Susumu Goto. Kegg: kyoto encyclopedia of genes and genomes. *Nucleic acids research*, 28(1):27–30, 2000.
- Thomas N Kipf and Max Welling. Semi-supervised classification with graph convolutional networks. *arXiv preprint arXiv:1609.02907*, 2016.
- Devin Kreuzer, Dominique Beaini, William L Hamilton, Vincent Létourneau, and Prudencio Tossou. Rethinking graph transformers with spectral attention. *arXiv preprint arXiv:2106.03893*, 2021.
- Alex Krizhevsky, Geoffrey Hinton, et al. Learning multiple layers of features from tiny images. 2009.
- Steffen L Lauritzen and David J Spiegelhalter. Local computations with probabilities on graphical structures and their application to expert systems. *Journal of the Royal Statistical Society: Series B (Methodological)*, 50(2):157–194, 1988.
- AA Leman and Boris Weisfeiler. A reduction of a graph to a canonical form and an algebra arising during this reduction. *Nauchno-Tekhnicheskaya Informatsiya*, 2(9):12–16, 1968.

- Xiaoxiao Li, Yuan Zhou, Nicha Dvornek, Muhan Zhang, Siyuan Gao, Juntang Zhuang, Dustin Scheinost, Lawrence H Staib, Pamela Ventola, and James S Duncan. Brainngn: Interpretable brain graph neural network for fmri analysis. *Medical Image Analysis*, 74:102233, 2021.
- Yaguang Li, Rose Yu, Cyrus Shahabi, and Yan Liu. Diffusion convolutional recurrent neural network: Data-driven traffic forecasting. *arXiv preprint arXiv:1707.01926*, 2017.
- Derek Lim, Joshua Robinson, Lingxiao Zhao, Tess Smidt, Suvrit Sra, Haggai Maron, and Stefanie Jegelka. Sign and basis invariant networks for spectral graph representation learning. *arXiv preprint arXiv:2202.13013*, 2022.
- Qiao Liu and Lei Xie. Transynergy: Mechanism-driven interpretable deep neural network for the synergistic prediction and pathway deconvolution of drug combinations. *PLoS computational biology*, 17(2):e1008653, 2021.
- Ying Lu and Jiawei Han. Cancer classification using gene expression data. *Information Systems*, 28(4):243–268, 2003.
- Haggai Maron, Heli Ben-Hamu, Hadar Serviansky, and Yaron Lipman. Provably powerful graph networks. *Advances in neural information processing systems*, 32, 2019.
- Brendan D McKay and Adolfo Piperno. Practical graph isomorphism, ii. *Journal of symbolic computation*, 60:94–112, 2014.
- Federico Monti, Michael M Bronstein, and Xavier Bresson. Geometric matrix completion with recurrent multi-graph neural networks. *arXiv preprint arXiv:1704.06803*, 2017.
- Christopher Morris, Martin Ritzert, Matthias Fey, William L Hamilton, Jan Eric Lenssen, Gaurav Rattan, and Martin Grohe. Weisfeiler and leman go neural: Higher-order graph neural networks. In *Proceedings of the AAAI conference on artificial intelligence*, volume 33, pp. 4602–4609, 2019.
- Ryan Murphy, Balasubramaniam Srinivasan, Vinayak Rao, and Bruno Ribeiro. Relational pooling for graph representations. In *International Conference on Machine Learning*, pp. 4663–4673. PMLR, 2019.
- Mathias Niepert, Mohamed Ahmed, and Konstantin Kutzkov. Learning convolutional neural networks for graphs. In *International conference on machine learning*, pp. 2014–2023. PMLR, 2016.
- Xiaoyong Pan and Hong-Bin Shen. Inferring disease-associated micrnas using semi-supervised multi-label graph convolutional networks. *Iscience*, 20:265–277, 2019.
- Pál András Papp and Roger Wattenhofer. A theoretical comparison of graph neural network extensions. In *International Conference on Machine Learning*, pp. 17323–17345. PMLR, 2022.
- Pál András Papp, Karolis Martinkus, Lukas Faber, and Roger Wattenhofer. Dropgnn: Random dropouts increase the expressiveness of graph neural networks. *Advances in Neural Information Processing Systems*, 34:21997–22009, 2021.
- Hieu Pham, Melody Guan, Barret Zoph, Quoc Le, and Jeff Dean. Efficient neural architecture search via parameters sharing. In *International Conference on Machine Learning*, pp. 4095–4104. PMLR, 2018.
- Scott H Podolsky and Jeremy A Greene. Combination drugs—hype, harm, and hope. *New England Journal of Medicine*, 365(6):488–491, 2011.
- Zhiwei Qin, Zhao Liu, and Ping Zhu. Aiding alzheimer’s disease diagnosis using graph convolutional networks based on rs-fmri data. In *2022 15th International Congress on Image and Signal Processing, BioMedical Engineering and Informatics (CISP-BMEI)*, pp. 1–7. IEEE, 2022.
- Raghunathan Ramakrishnan, Pavlo O Dral, Matthias Rupp, and O Anatole Von Lilienfeld. Quantum chemistry structures and properties of 134 kilo molecules. *Scientific data*, 1(1):1–7, 2014.
- Franco Scarselli, Marco Gori, Ah Chung Tsoi, Markus Hagenbuchner, and Gabriele Monfardini. The graph neural network model. *IEEE transactions on neural networks*, 20(1):61–80, 2008.

- Marco Scutari. Learning bayesian networks with the bnlearn r package. *Journal of Statistical Software*, 35(i03), 2010.
- Adam J Shuhendler, Richard Y Cheung, Janet Manias, Allegra Connor, Andrew M Rauth, and Xiao Yu Wu. A novel doxorubicin-mitomycin c co-encapsulated nanoparticle formulation exhibits anti-cancer synergy in multidrug resistant human breast cancer cells. *Breast cancer research and treatment*, 119(2):255–269, 2010.
- Tzu-An Song, Samadrita Roy Chowdhury, Fan Yang, Heidi Jacobs, Georges El Fakhri, Quanzheng Li, Keith Johnson, and Joyita Dutta. Graph convolutional neural networks for alzheimer’s disease classification. In *2019 IEEE 16th international symposium on biomedical imaging (ISBI 2019)*, pp. 414–417. IEEE, 2019.
- Veronika Thost and J. Chen. Directed acyclic graph neural networks. *ArXiv*, abs/2101.07965, 2021.
- Hannu Toivonen, Ashwin Srinivasan, Ross D King, Stefan Kramer, and Christoph Helma. Statistical evaluation of the predictive toxicology challenge 2000–2001. *Bioinformatics*, 19(10):1183–1193, 2003.
- Ashish Vaswani, Noam Shazeer, Niki Parmar, Jakob Uszkoreit, Llion Jones, Aidan N Gomez, Łukasz Kaiser, and Illia Polosukhin. Attention is all you need. In *Proceedings of the 31st International Conference on Neural Information Processing Systems*, pp. 6000–6010, 2017.
- Petar Velickovic, Guillem Cucurull, A. Casanova, Adriana Romero, P. Lio’, and Yoshua Bengio. Graph attention networks. *ArXiv*, abs/1710.10903, 2018.
- Archana Venkataraman, Daniel Y-J Yang, Kevin A Pelphrey, and James S Duncan. Bayesian community detection in the space of group-level functional differences. *IEEE transactions on medical imaging*, 35(8):1866–1882, 2016.
- Haorui Wang, Haoteng Yin, Muhan Zhang, and Pan Li. Equivariant and stable positional encoding for more powerful graph neural networks. *arXiv preprint arXiv:2203.00199*, 2022.
- Asiri Wijesinghe and Qing Wang. A new perspective on " how graph neural networks go beyond weisfeiler-lehman?". In *International Conference on Learning Representations*, 2022.
- Xiaohan Xing, Fan Yang, Hang Li, Jun Zhang, Yu Zhao, Mingxuan Gao, Junzhou Huang, and Jianhua Yao. Multi-level attention graph neural network based on co-expression gene modules for disease diagnosis and prognosis. *Bioinformatics*, 38(8):2178–2186, 2022.
- Keyulu Xu, Weihua Hu, Jure Leskovec, and Stefanie Jegelka. How powerful are graph neural networks? In *International Conference on Learning Representations*, 2019. URL <https://openreview.net/forum?id=ryGs6iA5Km>.
- Shen Yan, Yu Zheng, Wei Ao, Xiao Zeng, and Mi Zhang. Does unsupervised architecture representation learning help neural architecture search? *Advances in Neural Information Processing Systems*, 33, 2020.
- Chengxuan Ying, Tianle Cai, Shengjie Luo, Shuxin Zheng, Guolin Ke, Di He, Yanming Shen, and Tie-Yan Liu. Do transformers really perform bad for graph representation? *arXiv preprint arXiv:2106.05234*, 2021.
- Rex Ying, Ruining He, Kaifeng Chen, Pong Eksombatchai, William L Hamilton, and Jure Leskovec. Graph convolutional neural networks for web-scale recommender systems. In *Proceedings of the 24th ACM SIGKDD International Conference on Knowledge Discovery & Data Mining*, pp. 974–983, 2018.
- Jiaxuan You, Rex Ying, Xiang Ren, William Hamilton, and Jure Leskovec. Graphrnn: Generating realistic graphs with deep auto-regressive models. In *International Conference on Machine Learning*, pp. 5708–5717. PMLR, 2018.
- Jiaxuan You, Jonathan Gomes-Selman, Rex Ying, and Jure Leskovec. Identity-aware graph neural networks. *arXiv preprint arXiv:2101.10320*, 2021.

Muhan Zhang and Pan Li. Nested graph neural networks. *Advances in Neural Information Processing Systems*, 34, 2021.

Muhan Zhang, Zhicheng Cui, Marion Neumann, and Yixin Chen. An end-to-end deep learning architecture for graph classification. In *Proceedings of the AAAI Conference on Artificial Intelligence*, volume 32, 2018.

Muhan Zhang, Shali Jiang, Zhicheng Cui, Roman Garnett, and Yixin Chen. D-vae: A variational autoencoder for directed acyclic graphs. *Advances in neural information processing systems*, 32, 2019.

Lingxiao Zhao, Wei Jin, Leman Akoglu, and Neil Shah. From stars to subgraphs: Uplifting any gnn with local structure awareness. *arXiv preprint arXiv:2110.03753*, 2021.

Marinka Zitnik, Monica Agrawal, and Jure Leskovec. Modeling polypharmacy side effects with graph convolutional networks. *Bioinformatics*, 34(13):i457–i466, 2018.

A REPRESENTATION LEARNING TASKS ON GENE NETWORKS AND OTHER GRAPH BENCHMARKS

In the natural world, genes don’t operate independently and always function as part of a set of genes. Hence, they can be regulated as the graph modality based on reported genetic interactions that underlie phenotypes in a variety of bioinformatical systems. Then, various computational tasks on gene networks (graphs) are proposed in recent bioinformatics to numerically analyze contribution of genes to complex disease in humans. In this work, we take two long-standing challenging tasks in bioinformatics, Alzheimer’s disease (AD) classification and cancer subtype classification, as example, and introduces corresponding gene-network datasets. Here we compare the these gene network datasets against popular graph benchmark datasets to illustrate challenges of graph representation learning over gene networks.

Dataset	Ave. # nodes	Ave. # edges	# Tasks	Task Type	Metric
Mayo	3000	60000	2	Classification	Accuracy & F1
RosMap	3000	60000	2	Classification	Accuracy & F1
Cancer Subtype	3800	48000	7	Classification	Accuracy & F1
NA	8	12	1	Regression	RMSE & Pearson’s r
BN	10	15	1	Regression	RMSE & Pearson’s r
ogbg-molhiv	26	55	2	Classification	ROC-AUC
ZINC	23	50	1	Regression	MAE
D&D	284	1431	2	Classification	Accuracy
MUTAG	18	39	2	Classification	Accuracy
PROTEINS	39	146	2	Classification	Accuracy
PTC-MR	14	29	2	Classification	Accuracy
ENZYMES	33	124	6	Classification	Accuracy

Table 6: Comparison of gene networks and graphs in popular benchmark datasets

Table 6 presents preliminary results. Compared to graphs in popular benchmarks, gene networks always contain significantly large number of nodes (denoted as n) as well as the number of edges (denoted as m), which limits the applicability of popular expressive GNNs due to the complexity consideration. For subgraph-based GNNs like NGNN (Zhang & Li, 2021), the space complexity grows exponentially as the average node degree $\frac{m}{n}$ increases. For high-order GNNs, such as k-WL (Morris et al., 2019) and k-FWL (Grohe, 2021), that mimic the high-order WL algorithms, the stable colourings/representations can be computed in $\mathcal{O}(k^2 n^{k+1} \log n)$ with a space complexity of $\mathcal{O}(n^k)$. Consequently, it is hard to apply these methods to gene network representation learning.

B MORE DISCUSSION OF GC-GNN AND UGC-GNN

In this section, we provide more discussion of GC-GNN.

- **Part 1:** Limitations of GC-GNN and UGC-GNN.
- **Part 2:** The complexity of GC-GNN and UGC-GNN.

Part 1 (Table 7) One significant limitation of GC-GNN and UGC-GNN is that the (universal) graph canonization fail to consider the heterogeneity among edges. In addition, GC-GNN is also not guaranteed to be suitable for all graph learning tasks. Here we empirically test GC-GNN on molecular datasets, ogbg-molhiv and ogbg-molpcba, in Open Graph Benchmark (Hu et al., 2020). Table 7 provides empirical results. As we can see, GC-GNN still improve the performance over backbone GNNs and GC-GNN can achieve competitive performance to the powerful GNN baseline: ESAN with ED policy. However, we also notice that the improvement of GC-GNN is not significant as TU datasets and GC-GNN can not achieve the SOTA performance.

Part 2 The main concern of complexity comes from the graph canonization algorithms. As we discussed in the main paper (section 1.1, other related works), although graph canonization is a well-know NP-complete problem, practical canonization tools such as Nauty (McKay & Piperno, 2014) and Bliss (Junttila & Kaski, 2012), can effectively solve the problem in practice with an average time complexity of $\mathcal{O}(n)$. The process of computing the canonical forms of graphs can be implemented in

	ogbg-molhiv (AUC \uparrow)	ogbg-molpcba (AP \uparrow)
GCN (backbone)	0.7501 \pm 0.0140	0.2422 \pm 0.0034
ESAN (GCN + ED)	0.7559 \pm 0.0120	0.2521 \pm 0.0040
GN-GCN	0.7609 \pm 0.0158	0.2510 \pm 0.0047
GIN (backbone)	0.7744 \pm 0.0098	0.2703 \pm 0.0023
ESAN (GIN + ED)	0.7803 \pm 0.0170	0.2782 \pm 0.0036
GN-GIN	0.7705 \pm 0.0195	0.2781 \pm 0.0043

Table 7: Empirical results on molecular datasets.

the graph pre-process phase and we only need to perform practical graph canonization tools once for each graph. Furthermore, as the output discrete colouring $\{\rho(v_1|G), \rho(v_2|G) \dots \rho(v_n|G)\}$ of graph canonization are used as positional encodings of nodes, the additional space complexity is also $\mathcal{O}(n)$. Hence, compared to dominant expressive GNNs like subgraph-based GNNs and high-order GNNs, GC-GNN (UGC-GNN) is much more efficient with a significant low space and computation cost. For instance, on ogbg-molhiv, GC-GNN (GIN) takes 39 seconds per epoch, while Nested GIN takes 168 seconds.

C PROOF OF LEMMA 2.3 AND LEMMA 2.4

We first prove Lemma 2.3. Since discrete colouring $\{\rho(v_1|G), \rho(v_2|G), \dots, \rho(v_n|G)\}$ generated by graph canonization provides a unique way to label nodes for graphs in the same isomorphic group $ISO(G)$, then the isomorphism of two graphs can be determined by checking whether the node pairs of the same labels share the same edge relation. When the graph convolution layers on GNN g are injective, it can injectively map the pair of a node and the set of its' neighboring nodes. then if two graphs get different sets of learnt node embeddings by the GNN g , there must exists at least one pair of node label and the set of its' neighboring nodes' labels are different. Then, these two graphs are not isomorphic. On the other hand, when two graphs are not isomorphic, there must be at least one pair of nodes with the same labels, while the pair of nodes are connected in one graph yet disconnected in another graph. Then the graph convolution layer will output different embeddings for each node in the node pair.

Next, we prove Lemma 2.4 to support theoretical results about the stability of GNNs and GC-GNNs. Before proving our lemma, we first introduce some necessary preliminaries that we will later use in the proofs.

Preliminary 1: Decomposition of message passing layer of GNNs The message passing scheme adopted in popular GNNs iteratively updates a node's representation/embedding according to the multiset of its neighbors' representations/embeddings and its current representation/embedding. Let h_v^t denotes the representation of v in layer t , the message passing scheme is given by:

$$\begin{aligned} h_v^{t+1} &= \mathcal{M}(h_v^t, \{h_u^t | (u, v) \in E\}) \\ &= \mathcal{U}(h_v^t, \mathcal{A}(\{h_u^t | (u, v) \in E\})) \end{aligned}$$

Here, \mathcal{A} is an aggregation function on the multiset $S = \{h_u^t | (u, v) \in E\}$ and \mathcal{U} is an update function.

Definition C.1 A function f is claimed as a L -stable multiset function if 1) $\sum_{h \in S} f(h)$ is unique for each multiset S of bounded size; and 2) for any two multisets S_1 and S_2 , $\|\sum_{h \in S_1} f(h) - \sum_{h' \in S_2} f(h')\| \leq L \times d_S(S_1, S_2)$, where $d_S(S_1, S_2) = |S_1| + |S_2| - |S_1 \cap S_2|$.

The L -stable multiset function f provides a unique mapping between the multiset space and representation space, while distance between multisets in the representation space are bounded through the constant multiplier L .

Corollary C.2 Assume that input feature space \mathbb{H} is countable. Any message passing function \mathcal{M} over pairs (h, S) , where $h \in \mathbb{H}$ and $S \subset \mathbb{H}$, can be decomposed as $\mathcal{M}(h, S) = \phi((1 + \epsilon)f(h) + \sum_{h' \in S} f(h'))$ for some L -stable multiset function f , some function ϕ and infinitely many choices of ϵ .

This corollary C.2 can be obtained by following the Lemma 5 and Corollary 6 in Xu et al. (2019). Basically, since the space \mathbb{H} is countable, we can always get a mapping $Z : \mathbb{H} \rightarrow \mathbb{N}$ from $h \in \mathbb{H}$ to natural numbers. As S are bounded multiset, there always exists an upper bound B of their cardinality such that $|S| < B$ for any S . Hence, the example function $f(h) = B^{-Z(h)}$ satisfies both the uniqueness condition as well as the inequality condition in Definition C.1 where the constant $L = \frac{1}{B}$.

Preliminary 2: Graph canonization and individualization-and-refinement paradigm Here we provide an extended discussion on the graph canonization and individualization-refinement paradigm. To address the complex graph isomorphism/ graph canonization problem, practical graph canonization tools resort to the individualization-and-refinement paradigm, where the color refinement and individualization steps are iteratively performed to get a discrete colouring.

- 1. Color refinement step: The color refinement algorithm aims to recolor nodes in a graph by similarity. The algorithm starts with some initial node colors, then the algorithm updates node’s color round by round, and in each round, two nodes with the same color will get different new color if the multiset of neighboring colors are different. This process continues until an equitable colouring is obtained such that the node colors will not change even if another color refinement round happens.
- 2. Individualization step: When a stable colouring generated by the color refinement step is discrete, then returns a order of nodes in the canonical form. However, in many cases, the stable colouring are not discrete. Then the individualization step selects a node in a color class with more than one node and assigns a new (unseen) color to the node. Then the color refinement step is implemented again.

Specifically, in the color refinement step, the new colors are obtained by lexicographically sorting the pair of node current color and it’s multiset of neighboring colors. Hence, the new order of new node colors always follows that of the previous colors. That is, at round t , if two nodes v, u have different colors $c^t(u)$ and $c^t(v)$ such that $c^t(u) < c^t(v)$, then after one round of color refinement, the new colors of these two nodes have $c^{t+1}(u) < c^{t+1}(v)$.

Above individualization-refinement paradigm in practical graph canonization tools provide a solution to obtain a discrete coloring, yet not in a canonical way. That is, generated discrete coloring is not guaranteed to be the same for graphs in the same isomorphic class. To fix this, practical tools usually branch on all nodes of the same color in the individualization step and individualizes one node in each branch. Then a tree of colouring can be obtained such that each leaf of the tree is a discrete coloring of the input graph G . Then the final discrete colouring is selected, for example, as the leaf with the lexicographically minimal string that consists of the rows of the adjacency matrix according to the discrete colouring (i.e. node orders). More details can be found in McKay & Piperno (2014).

Proof. (Part one: A GNN model g is stable under X) Here, we assume the function ϕ in the decomposition of message passing layer of GNNs is K-Lipschitz. A function $\phi : (X, d_x) \rightarrow (Y, d_y)$ between two metric spaces is K-Lipschitz if $d_y(\phi(x_1), \phi(x_2)) \leq K d_x(x_1, x_2)$ for any $x_1, x_2 \in X$, where K is a constant.

Corollary C.3 *MLPs are K-Lipschitz.*

In popular message passing GNNs, ϕ is always modeled by a MLP. Hence, we need to prove corollary C.3 to use the K-Lipschitz assumption. For each MLP layer that characterized by the trainable parameter tensors W_i and b_i (bias), it can be represented as $\sigma(W_i x + b_i)$, where σ is the activation function. Then we have $\|\sigma(W_i x_1 + b_i) - \sigma(W_i x_2 + b_i)\| = \|\frac{\partial \sigma}{\partial x} W_i (x_1 - x_2)\|$. Since the activation function σ usually takes ReLU/sigmoid/tanh, it’s straightforward that $\|\frac{\partial \sigma}{\partial x}\|$ is bounded by a constant K_1 . Then we get $\|\frac{\partial \sigma}{\partial x} W_i (x_1 - x_2)\| \leq K_1 \|W_i\|_2 \|x_1 - x_2\|$, where $K_1 \|W_i\|_2$ is a constant independent of x_1 and x_2 . Hence, we show that MLPs are K-Lipschitz.

Next, let’s prove the theoretical result. Without loss of generality, we assume that the GNN contains a single message passing layer. For any two graphs $G^{(1)} = (A^{(1)}, X^{(1)})$ and $G^{(2)} = (A^{(2)}, X^{(2)})$, let $\pi^* \in \Pi(n)$ denotes the optimal permutation operation that best aligns the G_1 and G_2 , and P^* is the corresponding permutation matrix. Then we have,

$$\begin{aligned}
& \|g(A^{(1)}, X^{(1)}) - g(A^{(2)}, X^{(2)})\| \\
&= \left\| \sum_{v \in G^{(1)}} \phi((1+\epsilon)f(X_v^{(1)})) + \sum_{v' \in \mathcal{N}(v|G^{(1)})} f(X_{v'}^{(1)}) - \sum_{u \in G^{(2)}} \phi((1+\epsilon)f(X_u^{(2)})) + \sum_{u' \in \mathcal{N}(u|G^{(2)})} f(X_{u'}^{(2)}) \right\| \quad (1) \\
&\leq \sum_{v \in G^{(1)}} \left\| \phi((1+\epsilon)f(X_v^{(1)})) + \sum_{v' \in \mathcal{N}(v|G^{(1)})} f(X_{v'}^{(1)}) - \phi((1+\epsilon)f(X_{\pi^*(v)}^{(2)}) + \sum_{u' \in \mathcal{N}(\pi^*(v)|G^{(2)})} f(X_{u'}^{(2)}) \right\| \quad (2) \\
&\leq K \sum_{v \in G^{(1)}} \left\| (1+\epsilon)f(X_v^{(1)}) + \sum_{v' \in \mathcal{N}(v|G^{(1)})} f(X_{v'}^{(1)}) - (1+\epsilon)f(X_{\pi^*(v)}^{(2)}) - \sum_{u' \in \mathcal{N}(\pi^*(v)|G^{(2)})} f(X_{u'}^{(2)}) \right\| \quad (3) \\
&\leq K(1+\epsilon) \sum_{v \in G^{(1)}} \|f(X_v^{(1)}) - f(X_{\pi^*(v)}^{(2)})\| + K \sum_{v \in G^{(1)}} \left\| \sum_{v' \in \mathcal{N}(v|G^{(1)})} f(X_{v'}^{(1)}) - \sum_{u' \in \mathcal{N}(\pi^*(v)|G^{(2)})} f(X_{u'}^{(2)}) \right\| \quad (4) \\
&\leq K \times L \times (1+\epsilon) \left(\sum_v X_v^{(1)} \neq X_{\pi^*(v)}^{(2)} \right) + K \times L \times d_S(\mathcal{N}(v|G^{(1)}), \mathcal{N}(\pi^*(v)|G^{(2)})) \quad (5) \\
&\leq K \times L \times (1+\epsilon) d(G^{(1)}, G^{(2)}) \quad (6)
\end{aligned}$$

Here, we use the K-Lipschitz property in the step (4), and use the property of L-stable multiset function in step (6). Furthermore, $\mathcal{N}(v|G^{(1)})$ denotes the set of neighboring nodes of v in $G^{(1)}$, and can be characterized by the v th row of adjacency matrix $A^{(1)}$. $\mathcal{N}(\pi^*(v)|G^{(2)})$ denotes the set of neighboring nodes of v 's image in $G^{(2)}$, and can be characterized by the v th row of adjacency matrix $P^*A^{(2)}P^{*T}$. Hence, we show that GNN g is stable under X with a constant C of $K \times L \times (1+\epsilon)$.

Proof. (Part two: A GNN model g is not stable under $X \oplus P$) Here we provide a counter example. Let $G^{(1)}$ be a graph of n nodes such that 1) there is no node symmetry in the graph; 2) the node v_n has an initial color (integer feature) that is strictly larger than the colors of other nodes. Then, we obtain a graph $G^{(2)}$ by changing the initial color of node v_n in $G^{(1)}$ to another color which is strictly smaller than the colors of other nodes. Then, we know that there is no node symmetry in the graph $G^{(2)}$, either. Furthermore, it's straightforward that the best graph matching $\pi^* \in \Pi(n)$ between $G^{(1)}$ and $G^{(2)}$ is $\pi(i) = i$ for $\forall i = 1, 2, \dots, n$ and the corresponding permutation matrix $P^* = I$ is an identity matrix.

Since there is no node symmetry in $G^{(1)}$ and $G^{(2)}$, the color refinement step in graph normalization tools will generate discrete colourings for $G^{(1)}$ and $G^{(2)}$. Let $\{\rho(v_1|G^{(1)}), \rho(v_2|G^{(1)}), \dots, \rho(v_n|G^{(1)})\}$ and $\{\rho(v_1|G^{(2)}), \rho(v_2|G^{(2)}), \dots, \rho(v_n|G^{(2)})\}$ denote the corresponding discrete colourings. As we discussed in preliminary 2, the output discrete colouring from color refinement will keep the order of initial colors. Hence, we know that $\rho(v_n|G^{(1)}) = n$, $\rho(v_n|G^{(2)}) = 1$ and $\rho(v_i|G^{(1)}) = \rho(v_i|G^{(2)}) + 1$ for $i = 1, 2, \dots, n-1$. Thus, we get $\rho(v_i|G^{(1)}) \neq \rho(v_i|G^{(2)})$ for $i = 1, 2, \dots, n$, indicating that $P_v^{(1)} \neq P_v^{(2)}$ for $\forall v$. Thus, we have,

$$\begin{aligned}
& \|g(A^{(1)}, X^{(1)}) - g(A^{(2)}, X^{(2)})\| \\
&\geq \left\| \sum_{v \in G^{(1)}} (1+\epsilon)(f(X_v^{(1)} + P_v^{(1)}) - f(X_v^{(2)} + P_v^{(2)})) \right\| \quad (7)
\end{aligned}$$

$$\begin{aligned}
&\geq (1+\epsilon) \times |G^{(1)}| \times \frac{1}{B} \quad (8)
\end{aligned}$$

$$\begin{aligned}
&\geq 1 = d(G^{(1)}, G^{(2)}) \quad (9)
\end{aligned}$$

Since the function f is defined on the multiset whose cardinality is bounded by the overall graph size n , we get $B \leq |G^{(1)}|$.

D PROOF OF THEOREM 3.2

Proof. Following the proof of Lemma 2.4, we consider the same decomposition scheme $\mathcal{M}(h, S) = \phi((1+\epsilon)f(h) + \sum_{h' \in S} f(h'))$ of the message passing layer, yet the input space is $X \oplus P$ (where P is the 2-dimensional tensor of one-hot encodings of discrete colouring generated by universal graph normalization), instead of the input feature X .

Then, let's consider any pairs $\mathcal{N}(v|G^{(1)})$ and $\mathcal{N}(\pi^*(v)|G^{(2)})$. Since the discrete colouring in any common subgraph G' of $G^{(1)}$ and $G^{(2)}$ are identical, the number of same items in multisets $\{X_{v'}^{(1)}|v' \in \mathcal{N}(v|G^{(1)})\}$ and $\{X_{u'}^{(2)}|u' \in \mathcal{N}(\pi^*(v)|G^{(2)})\}$ will not change if we replace $X_{v'}^{(1)}$ with $X_{v'}^{(1)} + P_{v'}^{(1)}$, and $X_{u'}^{(2)}$ with $X_{u'}^{(2)} + P_{u'}^{(2)}$. Then we get,

$$\begin{aligned} & \sum_{v' \in \mathcal{N}(v|G^{(1)})} f(X_{v'}^{(1)} + P_{v'}^{(1)}) - \sum_{u' \in \mathcal{N}(\pi^*(v)|G^{(2)})} f(X_{u'}^{(2)} + P_{u'}^{(2)}) \\ = & \sum_{v' \in \mathcal{N}(v|G^{(1)})} f(X_{v'}^{(1)}) - \sum_{u' \in \mathcal{N}(\pi^*(v)|G^{(2)})} f(X_{u'}^{(2)}) \end{aligned} \quad (10)$$

Thus, we have

$$\begin{aligned} & \|g(A^{(1)}, X^{(1)}) - g(A^{(2)}, X^{(2)})\| \\ = & \left\| \sum_{v \in G^{(1)}} \phi((1 + \epsilon)f(X_v^{(1)} + P_v^{(1)}) + \sum_{v' \in \mathcal{N}(v|G^{(1)})} f(X_{v'}^{(1)} + P_{v'}^{(1)})) \right. \\ & \left. - \sum_{u \in G^{(2)}} \phi((1 + \epsilon)f(X_u^{(2)} + P_u^{(2)}) + \sum_{u' \in \mathcal{N}(u|G^{(2)})} f(X_{u'}^{(2)} + P_{u'}^{(2)})) \right\| \end{aligned} \quad (11)$$

$$\begin{aligned} \leq & K \sum_{v \in G^{(1)}} \left\| (1 + \epsilon)f(X_v^{(1)} + P_v^{(1)}) + \sum_{v' \in \mathcal{N}(v|G^{(1)})} f(X_{v'}^{(1)} + P_{v'}^{(1)}) \right. \\ & \left. - (1 + \epsilon)f(X_{\pi^*(v)}^{(2)} + P_{\pi^*(v)}^{(2)}) - \sum_{u' \in \mathcal{N}(\pi^*(v)|G^{(2)})} f(X_{u'}^{(2)} + P_{u'}^{(2)}) \right\| \end{aligned} \quad (12)$$

$$\begin{aligned} \leq & K(1 + \epsilon) \sum_{v \in G^{(1)}} \|f(X_v^{(1)} + P_v^{(1)}) - f(X_{\pi^*(v)}^{(2)} + P_{\pi^*(v)}^{(2)})\| \\ & + K \sum_{v \in G^{(1)}} \left\| \sum_{v' \in \mathcal{N}(v|G^{(1)})} f(X_{v'}^{(1)} + P_{v'}^{(1)}) - \sum_{u' \in \mathcal{N}(\pi^*(v)|G^{(2)})} f(X_{u'}^{(2)} + P_{u'}^{(2)}) \right\| \end{aligned} \quad (13)$$

$$\begin{aligned} = & K(1 + \epsilon) \sum_{v \in G^{(1)}} \|f(X_v^{(1)} + P_v^{(1)}) - f(X_{\pi^*(v)}^{(2)} + P_{\pi^*(v)}^{(2)})\| \\ & + K \sum_{v \in G^{(1)}} \left\| \sum_{v' \in \mathcal{N}(v|G^{(1)})} f(X_{v'}^{(1)}) - \sum_{u' \in \mathcal{N}(\pi^*(v)|G^{(2)})} f(X_{u'}^{(2)}) \right\| \end{aligned} \quad (14)$$

$$\leq K \times L \times (1 + \epsilon) d(G^{(1)}, G^{(2)}) \quad (15)$$

where we use the equation (11) in the step (14) to get step (15).

E PROOF OF LEMMA 3.3

Proof. Since the function $l(v|\mathbb{G}) : V \rightarrow \mathbb{N}$ is an injective function, it can distinguish nodes in each graph according to $l(v|\mathbb{G})$. Furthermore, since for $\forall v_1, u_1 \in G_1, v_2, u_2 \in G_2, G_1, G_2 \in \mathbb{G}$ such that $l(v_1|\mathbb{G}) = l(v_2|\mathbb{G})$ and $l(u_1|\mathbb{G}) = l(u_2|\mathbb{G})$, we have $(v_1, u_1) \in E_1 \leftrightarrow (v_2, u_2) \in E_2$, we know that the connectivity between node pairs (v, u) of the same label pairs $(l(v|\mathbb{G}), l(u|\mathbb{G}))$ is shared among all graphs. Let N be the total number of all potential different labels $l(v|\mathbb{G})$, then we can expand each graph to a larger graph of size N , where each node v has an order/position of $l(v|\mathbb{G})$, and rest positions are padded by dummy nodes that is not connected with any other nodes. Then, any common subgraph G' of G_1 and G_2 , is also a common subgraph of their converted larger graphs, and it is obvious that the orders of nodes in each common subgraph of these generated larger graphs are identical.

F PROOF OF LEMMA 3.4

Proof. Let $G = (A, X)$ be an arbitrary graph of size n , and $\forall P \in \Pi(n)$ where $\Pi(n)$ is the permutation group. $\{l(v_1|\mathbb{G}), l(v_2|\mathbb{G}) \dots l(v_n|\mathbb{G})\}$ is the discrete colouring of G generated by the

universal graph canonization. The discrete colouring is invariant to the permutation operation P as graphs from the same isomorphic class has the same canonical form (so as the same output discrete colouring from universal graph canonization). Here, we use L to denote a 2-dimension tensor of one-hot features of this discrete colouring. Then, let $G' = (PAP^T, PX)$ (G' is isomorphic to G), then, the corresponding discrete colouring tensor is PL . Let \mathcal{M} be a stack of message passing layers, then we have $P\mathcal{M}(A, X) = \mathcal{M}(PAP^T, PX)$ for $\forall X, A$. Let \mathcal{R} denote the readout function of UNGNN, that is $\mathcal{R}(\{h_v|v \in V\}) = \sum_{v \in V} W_{l(v|\mathbb{G})}h_v$, then \mathcal{R} is invariant to the order of $\{h_v|v \in V\}$ as the corresponding weight matrix $W_{l(v|\mathbb{G})}$ is solely decided by node’s discrete color $l(v|\mathbb{G})$. Hence, UNGNN g is a composition of functions \mathcal{R} and \mathcal{M} , then we get:

$$\begin{aligned} g(PAP^T, PX) &= \mathcal{R}(\mathcal{M}(PAP^T, PX + PL)) \\ &= \mathcal{R}(\mathcal{M}(PAP^T, P(X + L))) \\ &= \mathcal{R}(P\mathcal{M}(A, X + L)) \\ &= \mathcal{R}(\mathcal{M}(A, X + L)) = g(A, X) \end{aligned}$$

G MORE ABLATION RESULTS

Methods	Mayo		RosMap		Cancer Subtype	
	Accuracy \uparrow	F1 score \uparrow	Accuracy \uparrow	F1 score \uparrow	Accuracy \uparrow	F1 score \uparrow
GIN	0.496 \pm 0.042	0.484 \pm 0.036	0.471 \pm 0.039	0.482 \pm 0.041	0.537 \pm 0.045	0.512 \pm 0.047
GCN	0.561 \pm 0.049	0.535 \pm 0.021	0.520 \pm 0.036	0.571 \pm 0.032	0.593 \pm 0.039	0.561 \pm 0.042
GIN + GC	0.483 \pm 0.026	0.472 \pm 0.031	0.486 \pm 0.041	0.510 \pm 0.037	0.539 \pm 0.041	0.532 \pm 0.069
GCN + GC	0.522 \pm 0.019	0.539 \pm 0.031	0.508 \pm 0.032	0.527 \pm 0.031	0.544 \pm 0.025	0.582 \pm 0.042
GIN + UGC	0.561 \pm 0.027	0.570 \pm 0.031	0.697 \pm 0.041	0.624 \pm 0.037	0.589 \pm 0.041	0.562 \pm 0.069
GCN + UGC	0.572 \pm 0.021	0.619 \pm 0.037	0.658 \pm 0.030	0.621 \pm 0.021	0.619 \pm 0.025	0.581 \pm 0.031
UGC-GNN (GIN)	0.624 \pm 0.036	0.713 \pm 0.022	0.701 \pm 0.025	0.689 \pm 0.019	0.714 \pm 0.011	0.701 \pm 0.032
UGC-GNN (GCN)	0.603 \pm 0.031	0.652 \pm 0.020	0.724 \pm 0.021	0.697 \pm 0.019	0.691 \pm 0.013	0.706 \pm 0.029

Table 8: Ablation study results. GC = graph canonization, UGC = universal graph canonization. **Best results** are highlighted.

Ablation study results. Table 8. This experiment tests the effectiveness of different components in UGC-GNN and empirically supports theoretical findings in the paper. When comparing GIN (GCN), GIN + GC (GCN + GC), and GIN + UGC (GCN + UGC), (1) we find GNNs with general graph canonization usually causes the decrease of the testing performance (i.e. GIN + GC < GIN, GCN + GC < GCN). This finding aligns well with Lemma 2.4, indicating that stability of GNN is of great practical importance in real datasets especially when graphs are large. (2) We also observe that GNNs with universal graph canonization significantly enhance the model performance, and the observation empirically supports the Lemma 3.3. Furthermore, we also find that GIN (GCN) < GIN + UGC (GCN + UGC) < and UGC-GNN (GIN or GCN). Consequently, the canonical information from the discrete colouring $\{l(v_1|\mathbb{G}), l(v_2|\mathbb{G}) \dots l(v_n|\mathbb{G})\}$ enhance the base GNN architecture from the perspective of both message passing process and the readout function.

H GRAPH STRUCTURED DATA IN BIOINFORMATICS AND THEIR GNN BASELINES

The dominant graph-structured biological data in bioinformatics can be categorized into three types: (1) molecular graphs, (2) biological interaction graphs and (3) gene networks/graphs. Different types of these biological graph data have different SoTA GNN baselines.

In molecular graphs, atoms or other chemical compounds are used as nodes, and the bonds are formulated as the edges. Molecular graphs are homogeneous graphs and are widely used as benchmark datasets in the field of representation learning on graphs and GNNs (graph neural networks). Typical molecular graph benchmark datasets include ZINC, QM9 Ramakrishnan et al. (2014), Molhiv in OGB (Open Graph Benchmark), etc. Dominant baseline deep learning models for these molecular graph datasets are popular GNN models, such as GIN, GCN, GINE, NGNN, PPGN, and these baselines are used in our experiments.

In biological interaction graphs, nodes represent genes, drugs, disease, RNA, etc, and an edge indicates the existence of a known association between entities connected by the edge. Thus, biological interaction graphs are heterogeneous graphs. Typical biological interaction graphs include gene-drug interaction networks in the drug synergy prediction task, drug-protein interaction networks Zitnik et al. (2018) in side effect prediction tasks, and miRNA-disease interaction networks Pan & Shen (2019) in the disease classification task. For the representation learning tasks on biological interaction graphs, various task-specific graph neural networks are proposed, and here we provide some popular examples: TransSynergy Liu & Xie (2021) and SANEpool Dong et al. (2023) for gene-drug interaction networks; Decagon for drug-protein interaction networks; and DimiG Pan & Shen (2019) for miRNA-disease interaction networks. Overall, these task-specific GNNs focus more on how to effectively construct the biological interaction graphs and represent initial features related to genes/drugs/ disease/RNA. Instead of the architecture design of GNNs. Consequently, these task-specific GNNs may not be well generalized to other graph learning tasks such as the gene network representation learning. In the paper, we select TransSynergy, SANEpool, Decagon and DimiG as baselines, and compare them with the proposed UGC-GNN.

In gene graphs/networks, genes are used as nodes, and an edge is used to link two genes if there is a physical signaling interaction between the genes from the documented medical experiment. Similar to molecular graphs, gene graphs/networks are also homogeneous graphs. Very limited works are proposed for gene network representation learning. MLA-GNN is proposed for graph-level classification tasks on gene networks, thus it can be used as a good baseline in the field.

I COMPUTATION EFFICIENCY

In this experiment, we compare the of computation cost of GNNs enhanced by graph canonization techniques (UGC-GNN) against dominant expressive GNNs to emphasize the advantage in efficiency.(1) For high-order GNNs, PPGN has a space complexity of $\mathcal{O}(n^2)$ for each layer, while 1-2-3 GNNs has a space complexity of $\mathcal{O}(n^3)$ for each layer. Then, when we test 1-2-3 GNN on Mayo, RosMap and Cancer, 1-2-3 GNNs always meet the OOM (out-of-memory) problem . On the other hand, by reducing the embedding dimension and number of layers, PPGN can avoid OOM problem on these datasets as Table 3 in the main paper indicates; (2) For subgraph-based GNNs like NGNN (nested GNN), we also implement the similar strategy to restrict the radius of subgraphs to be smaller than 2, then NGNN can avoid the OOM problem, too. Consequently, here we compare the average computation time per epoch of UGC-GNN against NGNN and PPGN on large-scale datasets.

	Mayo	RosMap	Cancer
NGNN	48s	42s	334s
PPGN	143s	126s	1261s
UGC-GNN (GIN)	13s	10s	89s

Table 9: Average computation time per epoch.

Table 9 demonstrates the experimental results. First, we find that UGC-GNN significantly reduces the computation complexity compared to high-order GNN PPGN, and this observation can be explained by the $\mathcal{O}(n^3)$ time complexity of PPGN and the large size of graphs. On the other hand, NGNN suffers from large subgraph sizes caused by the large average node degree in these datasets, then the extra computation burden is also larger than popular graph datasets with small average node degree (like OGB and TU datasets).

In addition, we need to point out that ESAN with EGO and EGO+ policy can be considered as a subgraph-based GNN. However, when the node-deleted subgraphs (ND) and the edge-deleted subgraphs (ED) polices are used, a graph is mapped to the set of subgraphs obtained by removing a single node or edge, then ESAN can be understood through the marking prism. In our experiments, ESAN is equipped with ED policy.